Transactions, SMiRT-22
San Francisco, California, USA - August 18-23, 2013
Division 5

A MODELING METHODOLOGY IN PREDICTING THE LEAKAGE TIGHTNESS OF A PRESSURE CONTAINMENT VESSEL WITHOUT LINER

Mahsa Mozayan Kharazi[1], Luc Davenne[2], and Shahrokh Ghavamian[3]

[1] Phd student, LMT Cachan and NECS, France (mmk@necs.fr)
[2] Assistant professor, Université Paris Ouest, Nanterre La Défense, France
[3] General Manager, NECS, Sceaux, France

ABSTRACT

The purpose of this paper is to present a complete analysis tool and numerical modeling methodology developed to help engineers studying the behavior of a prestressed concrete pressure containment vessel (PCCV) without liner of a nuclear power plant (NPP). Here the quantity of gas flow through concrete wall is separated in three parts: leakage through natural porosity of concrete; accelerated flow through micro-cracks and macro-cracks. Transport through the unsaturated sound and micro-cracked concrete is calculated by Darcy's law. In presence of macro-cracks, it is with Poiseuille-flow equation that leakage is represented. Gas transfer equations are solved by analogy to thermal equations. Gas permeability in each zone is determined as a function of the thermo-hydric and mechanical states of concrete; which require primary uncoupled thermo-hydric and mechanical analyses. Calculations including moisture and heat transfer, concrete creep, shrinkage, damage and cracking. Finally, this uncoupled thermo-hydro-mechanical methodology has been developed in Code_Aster finite elements code (EDF) to study the leakage tightness behavior of full scale PCCV. Different experimental elementary tests are studied to check the validity of mechanical, thermal, moisture flow and hydraulic models individually and when coupled together. A large-scale structural application is also presented here in order to assess the model's ability to simulate a full scale structure with all its complexity. The reasonable computation time, the stability of the numerical model and the quality of results, which follow the expected trends, constitute the assets of this tool and methodology to perform industrial studies.

INTRODUCTION

One of the main functions of a pressure containment vessel is its capacity to provide sufficient leakage tightness. This could be obtained either by placing a liner covering the entire surface of the vessel, or by a thicker reinforced concrete wall. Periodically, the tightness of containments vessels is measured by means of Structural Integrity Tests (SIT), by pressurizing the vessel. In most cases, test results are positive with leakage rates constant over the time. However, leakage measures indicate an increased rate in time. The reasons are more or less well known. The purpose of this paper is to present a modeling set accompanied by a study methodology to help engineers investigate some of those mechanisms involved in leakage tightness degradation of pre-stressed reinforced concrete pressure containment vessels without liner. An important feature of this work is that the solution proposed is suitable to study full size reactor buildings. Most research work dealing with this matter propose sophisticated modeling techniques, but their complexity and cost (model preparation and computation) make it that they are only suitable for local studies. It is essential to simultaneously encounter all phenomena behind leakage tightness decay, in order to be able to compare simulation results with test measures and observations. This is mandatory to demonstrate the efficiency of the technique, in order to provide engineers with reliable prediction analysis tools that can be used to improve design codes for future constructions, or develop retrofitting solutions to improve or maintain leakage tightness of existing reactor buildings.

METHODOLOGY

In the methodology proposed by this work, the gas flow across a concrete wall is classified in three parts: flow due to the natural porosity of material; accelerated flow through micro-cracks, and flow through macro cracks. In the last case, both open and reclosed cracks are accounted for. In this approach, it is considered that the gas phase consists only of dry air. Transport through the unsaturated sound concrete, micro-cracked concrete and reclosed cracks is calculated by Darcy's law. In case of discrete open cracks, it is with Poiseuille-flow equation that leakage is estimated. All necessary models and resolution strategy are implemented in Code_Aster® (EDF) finite elements program.

The gas transfer equations are solved by analogy to thermal equations. To predict the gas transfer through unsaturated sound, damaged and cracked concrete, the gas permeability in these different zones are needed. In unsaturated sound concrete, gas permeability is defined by both intrinsic porosity and hydric state of concrete (degree of saturation). In unsaturated damaged and reclosed cracked concrete, permeability depends on both hydric state (degree of saturation) and mechanical state (damage) of concrete. For cracked concrete, the permeability depends on the mechanical state (crack width). That is why, prior to permeability and leakage calculations, thermo-hydric and mechanical analyses should be performed to determine saturation degrees, damage states of concrete, and crack state (reclosed or open and their opening). In our approach, the different computations are uncoupled. The mechanical degradation is defined independently from the drying effect. In the mechanical model, the aging effect of the concrete is taken in account using a non-linear creep model. Then damage and crack-openings are calculated by post-processing the mechanical state of concrete.

Once the mechanical state and hydric state of concrete are known, a gas permeability distribution is calculated. Using the gas permeability, hydraulic conductivity is calculated and then included in the gas transfer equations to simulate the gas pressure gradient. This approach supposes the following hypothesis. First, damage does not influence the evolution of the saturation degree and vice versa. Mechanical and hydric properties are here totally uncoupled. Secondly, during the gas pressure loading, water saturation and damage do not evolve. In the first part of this contribution, the theoretical framework of hydraulic model is presented. Second part focuses on the thermo-hydric and mechanical calculations. Next, the numerical implantation and some experimental validation and parameter identification are also presented to determine the validity domain of hydraulic model. Finally, a large-scale structural application is studied in order to assess the model's ability to simulate a complex case. Several parametric analyses are carried out to determine their influence.

THEORETICAL FRAMEWORK OF HYDRAULIC MODEL

Sound and micro-cracked areas

The simulation of gas transport through a partially saturated porous medium is based on the resolution of three mass balance equations (Bear, 1991). Assuming that the gaseous phase does not contain water vapor and considering the gas transport only, the corresponding mass balance equation can be written as follows (Jason, 2001):

$$\frac{\partial}{\partial t}\left(\varphi\rho_g(1-S_l)\right) = -div(\varphi(1-S_l)\rho_g v_g) \tag{1}$$

With φ total porosity, ρ_g the mass density, v_g velocity of gas and S_l the degree of saturation:

$$S_l = \frac{C}{C_{sat}} \qquad with \quad C_{sat}\,(l/m^3) = 1000\,\phi \tag{2}$$

C is the volumetric water content and C_{sat} the water content for saturated sample.
The gas velocity in the sound and micro-cracked concrete is obtained using Darcy law for a partially saturated porous medium:

$$\phi(1-S_l)v_g = -\frac{K_g}{\eta_g} grad(P_g) \tag{3}$$

Where K_g is the gas permeability, η_g associated dynamic viscosity and P_g gas pressure. Using the Darcy law (Equation(3)) and considering the assumption of "ideal" gases, Equation (1) is rearranged as follow:

$$(1-S_l)\varphi\frac{\partial P_g}{\partial t} = -div(-\lambda_{NC}(P_g)\, grad\,(P_g)) \quad with \quad \lambda_{NC}(P_g) = \frac{K_g}{\eta_g}P_g \tag{4}$$

Where λ_{NC} is the non-linear uncracked "diffusive" conductivity. Equation (4) resembles nonlinear thermal equation (nonlinear because λ_{NC} depending on P_g). λ_{NC} involves the definition of the gas permeability in the partially saturated sound and damaged concrete.

$$K_g = K_g(\phi, S_l, D)$$

Where D is diffusive damage. Once the hydraulic equation is solved, macroscopic gas velocity is post-processed with:

$$\overline{v_g} = -\frac{K_g}{\eta_g} grad\,(P_g) \tag{5}$$

From Equation (5) the gas leakage could be deduced.

To obtain the total gas permeability in the partially saturated sound and micro-cracked zone the decomposition proposed by Baroghel-Bouny et al. (1999) is used. The total gas permeability K_g is split into two terms:

$$K_g(\varphi, S_l, D) = k_{rg}(S_l).K(\varphi, D) \tag{6}$$

With k_{rg} the relative gas permeability, which is a function of the saturation degree (S_l), and K [m^2] the absolute permeability, which is a function of the intrinsic property of pore structure (φ) and mechanical damage (D).This separation enables to simplify the problem by uncoupling the drying and mechanical effects on the material permeability. It relies on a condition between k_{rg} and the saturation degree (S_l) and another one between K(φ, D) and mechanical state (φ, D) for dried concrete.

In this work, relative permeability expression suggested by Verdier (2001) and based on modified Van Genuchten model (Van Genuchten, 1980, Monlouis-Bonnaire et al., 2003) is used:

$$k_{rg}(S_l) = \sqrt{(1-S_l)}\ .(1-S_l^{\frac{1}{b}})^{0.5b} \tag{7}$$

The advantage of this expression is that it does not underestimate the permeability for high water degrees of saturation (Jian LIU, 2011), contrary to other solutions proposed in the literature. Here b is considered equal to 2.9 from the experimental results.

The intrinsic gas permeability in the sound concrete depends only on the porosity of concrete. But if concrete is damaged permeability increses due to the presence of microcraks. To take into account the influence of micro cracking on gas permeability evolution, different empirical models have been proposed (Picandet et al., 2001, Souley et al., 2001, Gawin et al. 2003). One should notice that all thse experimental programs measure permeability evolution through compressive tests. In case of containement vessels, microcraking is mostly created by traction. For the purpose of our work we started with the model proposed by Picandet et al. (2001):

$$K(\varphi, D) = K_0 \exp\left\lfloor \left(\alpha \times D\right)^{\beta} \right\rfloor \tag{8}$$

Using data from an expeimental campagn based on the compression of cylindrical specimens, α and β constants were identified having values of 11.3 and 1.64 respectively. This law is valid for damage index D values ranging from 0 to 0.18. As mentioned, these were compressive tests, where D represents the change in material stiffness:

$$D = \frac{E_0 - E_D}{E_0} \tag{9}$$

where E_0 is the initial Youns modulus, E_D the unloagin stiffness.The direct application of this model for direct tensile conditions without precaution would overestimate permeabity compared to other experimental observations (Aldea et al, 1998, Gérard, 1996, Wang et al., 1997, Desmettre and Charron, 2011). To adapt the model to direct tensile cracking of concrete, the definition of the governing evolution variable ε_{eq} (equation (17)) is modified to $\varepsilon_{eq} = -\sqrt{2} \times \nu \times \varepsilon$, where ε represents the uniaxial compressive strain. The Picandet model can then be rewritten as follow:

$$K(\varphi, D) = K_0 \exp\left[\left(11.3 \times \sqrt{2} \times \nu \times D\right)^{1.64}\right] \qquad for \quad D < D_{\lim} \tag{10}$$

From experimental measures with specimen under tension, we notice that this formulation is valid for damage values bellow 0.2 ($D_{\lim}$). For damage value exceeding this limit, macro-cracks appear and gas transfer can no longer be considered as a diffusive phenomenon, which required the modification of equations, 1 and 3.

Macro-cracked areas

Mass balance equation through the macro-cracks is modified as follow (Bear, 1999):

$$\frac{\partial}{\partial t}\left(\rho_g\right) = -div(\rho_g v_g) \tag{11}$$

The gas velocity through N_c cracks is obtained using Poiseuille law instead of Darcy law:

$$v_g = -\frac{N_c \xi w_c^2}{12\eta_g} grad(P_g) = -\frac{K_g(w_c)}{\eta_g} grad(P_g) \tag{12}$$

Where N_c is the number of cracks, ξ is the flow coefficient, w_c average crack opening and $K_g(w_c)$ is the gas permeability through cracks. Using the Piseuille law (equation (12)) and considering the assumption of "ideal" gas condition, equation (11) can be rearranged as follow:

$$\frac{\partial P_g}{\partial t} = -div(-\lambda_C(P_g)\, grad\,(P_g)) \quad with \quad \lambda_C(P_g) = \frac{K_g(w_c)}{\eta_g} P_g \tag{13}$$

In order to apply this equation to an elementary volume (V_t) containing N_c cracks with a volume equal to V_c, a geometrical coefficient (γ) is applied:

$$\gamma \times \frac{\partial P_g}{\partial t} = -div(-\gamma \times \lambda_C(P_g)\, grad\,(P_g)) \qquad with \quad \gamma = \frac{V_c}{V_t} \tag{14}$$

The macroscopic gas velocity in the cracked concrete is then estimated by:

$$\overline{v_g} = -\gamma \times \frac{K_g}{\eta_g} grad\,(P_g) \tag{15}$$

In this work the gas transfer through the reclosed crack is modeled by Darcy law (similar to the equation(4)) with $K_g = K_g(\phi_{cc}, S_l)$ where φ_{cc} is close crack porosity.

THERMO-HYDRO-MECHANICAL CALCULATION

Thermo-hydric calculations

The distribution of water content is obtained by means of a moisture flow analysis:

$$\frac{\partial C}{\partial t} = -div(-D(C,T)\, grad(C)) \tag{16}$$

With D(C, T) the non-linear diffusive coefficient (Granger, 1994) function of the water content C, and temperature T. The temperature distribution is obtained from a prior thermal analysis.

Mechanical Calculations

In long-term behaviour of large-scale structures such as PCCV, creep is considered to be one of the principal causes for concrete damage. Concrete creep may lead to partial reduction of pre-stressing and in extreme cases consequently expose concrete to tensile stress state. Most creep models (Bazant 1983, Granger 1995) are developed for uni-axial stress states. Some authors such as Benboudjema (2002) and Kim et al (2006) generalized uniaxial creep models to multi axial. Since the concrete wall of pressure containment vessel is under biaxial stress states, our choice was made for Benboudjema's model. In this work, in order to evaluate damage, a simplified post-processing method based on Mazars' model (Mazars, 1984) has been developed. The evolution of damage is controlled by the so-called equivalent strain that characterizes the material extension during loading:

$$\varepsilon_{eq} = \sqrt{\langle \breve{\varepsilon}_1 \rangle_+^2 + \langle \breve{\varepsilon}_2 \rangle_+^2 + \langle \breve{\varepsilon}_3 \rangle_+^2} \tag{17}$$

$\langle \varepsilon_i \rangle_+$ is the positive strain value in the principal i direction. The strain tensor, which is used to calculate the equivalent strain, is given by the following equation:

$$\underline{\underline{\breve{\varepsilon}}} = \underline{\underline{\varepsilon}}^{elastic} + \chi \underline{\underline{\varepsilon}}^{creep} \qquad 0 < \chi < 1 \tag{18}$$

χ is the coupling creep-damage coefficient. It should be noted that our approach is sequential and damage index D does not modify the mechanical state of the structure. Comparing to nonlinear creep-damage model in the literature, this post-processing method is more robust and efficient for large-scale applications with moderate damage.

For leakage analysis, when damage exceeds D_{lim}, we consider gas flow through macro-cracks. Relying on a simplified method, the crack spacing (e_c) is determined using Eurocode standard. From e_c the crack opening is computed using the strain tensor. For an elementary volume containing N_c cracks in the direction of main positive principle strain, the crack opening is obtained as follow:

$$w_c = \frac{\int \breve{\varepsilon}\, dl}{N_c} \tag{19}$$

In the case that the strain integral becomes negative, the crack is considered to be closed. If crack opening is simultaneously positive for both principal directions, then the sum of openings is considered.

NUMERICAL IMPLEMENTATIONS AND EXPERIMENTAL VALIDATIONS

Damage, crack and hydraulic models are implemented in *Code_Aster*®. To improve the regularity of the transient solution, *hydraulic mass matrix* is lumped and an implicit finite difference time integration scheme (θ method, with θ=1) is adopted. Different parameter identifications and physical validation tests are presented in the following table:

Table 1: Identification and validation tests.

Identification / Validation	Model	Reference
Creep model parameters	Mechanical	Recordings from monitoring system incorporated in the structure
Crack spacing	Mechanical	Experimental tensile tests of RC beams (Mivelaz, 1996) - Experimental tensile test of RC specimen (Desmettre and Charron, 2011)
Moisture flow model	Drying	Mass loss experimental test (Granger, 1995, Verdier, 2001)
Relative gas permeability $k_{rg}(Sl)$ model	Hydraulic	Experimental relative gas permeability tests (Villain et al 2001, Abbas et al, 1999, Baroghel et Bouny, 1999)
Absolute permeability model $k(\varphi,D)$ and D_{lim}	Hydraulic	Experimental compression test (Kermani, 1991, Piccandet ,2009, Choinska et al, 2007, Hearn et al, 1998, Sugiyama et al., 1996) - Splitting test (Wang et al. 1997, Aldea et al 1998,

		Picandet, 2009) - Experimental tensile test of RC specimens (Desmettre and Charron , 2011)
Gas flow through cracks	Hydraulic	Splitting test (Wang et al. 1997, Aldea et al 1998, Picandet, 2009)
Diffusive and through crack gas flow	Hydraulic	Experimental tensile test of RC specimen (Desmettre and Charron, 2011)

LARGE-SCALE STRUCTURAL APPLICATION

As mentioned before, an important feature of this work is that the solution proposed is adapted to the study of full size engineering application, and more specifically NPP reactor buildings. Here the application concerns the study of PCCV without liner. The analysis is carried out for a period of 60 years. In the analysis, leakage tests carried out every 10 years is also considered. The internal test relative pressure is 0.38 MPa (Figure 3). The evolution of mechanical state, drying state and hydraulic state of the vessel are then computed. The aging effect is also taken into account using a non-linear creep model. The creep model parameters are calibrated to simulate a hypothetical situation. In this work the results of the last integrity test (IT5) are presented. FEM meshing of the reactor buildings is shown in Figure 1. Figure 2 shows pre-stressing tendons layout.

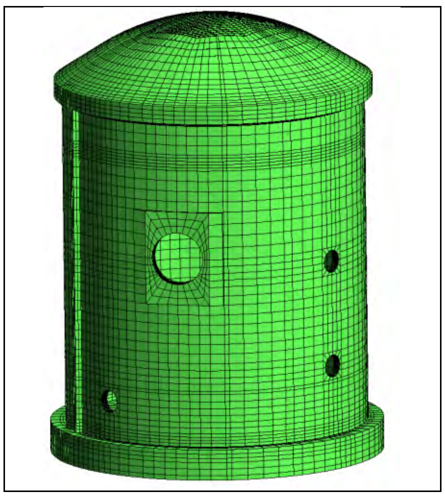

Figure 1. Geometry and mesh of the vessel

In determining soil-structure interaction, the structure is considered to be built on a hard soil. Soil and concrete part of the vessel are represented by solid elements. Prestressing tendons are modeled by 2-node truss elements.

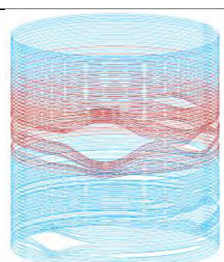	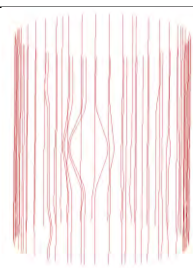		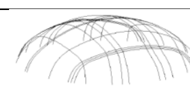
Hoop tendons	Vertical tendons	Gamma tendons	Dome tendons

Figure 2. Prestressing tendons

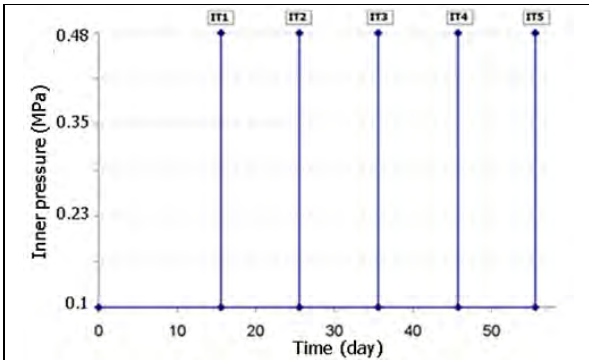

Figure 3. Integrity tests program over 60 years

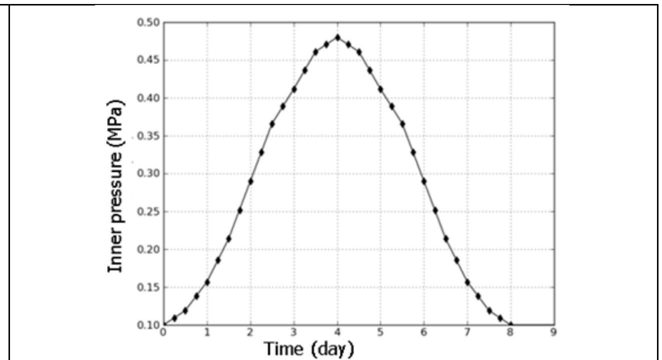

Figure 4. Pressure evolution during an integrity test

As an example, Figure 5 and Figure 6 represent temperature and degree of water saturation in concrete. The boundary conditions are expressed in terms of air temperature and humidity flow on internal and external surfaces (Granger, 1994). On Figure 6 it can be observed that the outer surface of the vessel dries more that the inner surface.

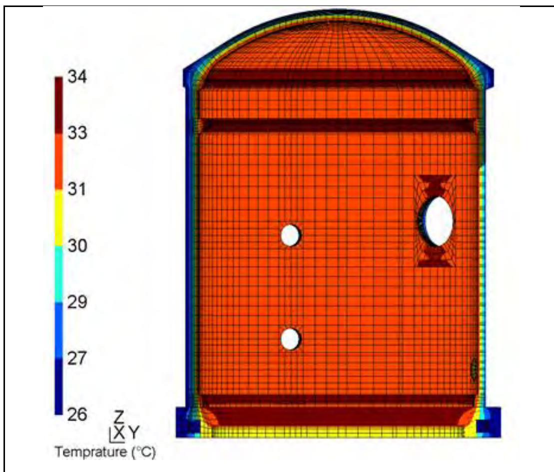

Figure 5. Thermic results (t= IT5)

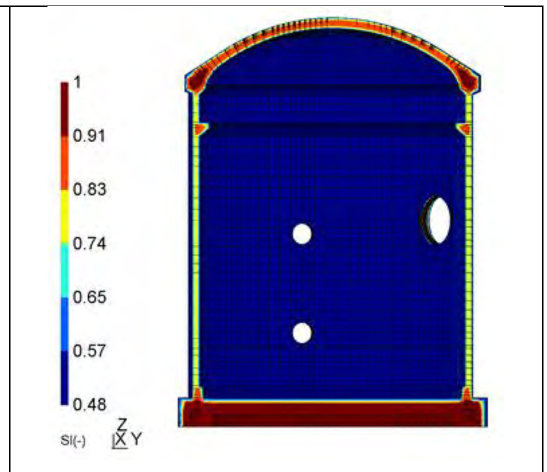

Figure 6. Drying results(t= IT5)

Figure 7 represents the damage distribution over the outer surface of the vessel. Important damage values are observed around the cylinder wall junction areas with the dome and basement, and close to hatch openings. In some regions, damage progresses deep inside the wall thickness. This is due to tensile stress concentration and loss of prestressing. Areas with damage index above D_{lim}, considered as cracking are indicated in Figure 8. These are categorized in open and closed cracks.

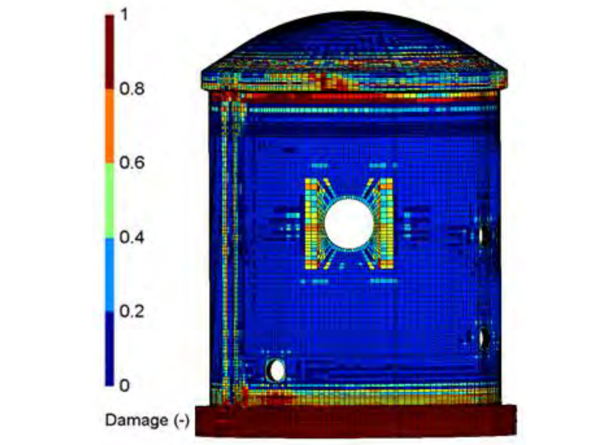

Figure 7. Damage results (t= 4th day of IT5)

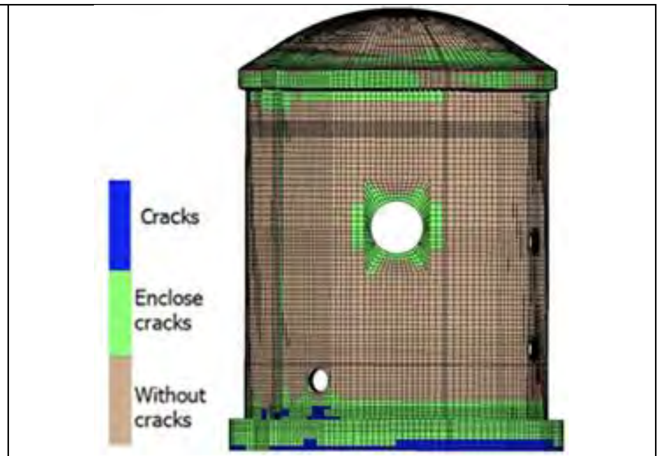

Figure 8. Cracking results(t= 4th day of IT5)

Once the damage, cracking, and saturation distributions are known, the local permeability and consequently the hydraulic conductivity are calculated by equations (4) and (14). The hydraulic boundary conditions are as follows: an atmospheric pressure is applied on both inner and outer surfaces of the vessel during all its lifetime (0.1 MPa). During integrity tests, a relative gas pressure (Figure 3) is also applied to the inner surface. Figure 9 and Figure 10 illustrate the normalized macroscopic gas velocity passing through the inner and outer faces of the at the 4th day of the 5th integrity test Figure 11 illustrates the flow into the wall at the inner side and out of the wall through the outer side of the wall during the test. Here, integrity test lasts 8 days. The internal pressure reaches its maximum value of 4.8 MPa at the 4th day before decreasing to its initial value of 0.1 MPa (Figure 3). Figure 11 illustrates that the internal wall normalized gas flow entering the wall reaches its maximum value also on the 4th day. After the 6th day, part of the air stored in the wall during the first days tends to find its way out. Since the core of the wall remains highly saturated with low relative gas permeability, it is easier for the gas to re-enter the vessel building (negative values of internal flow in Figure 11). In this study we can see that despite the increase in permeability of concrete wall, the container maintains most of its leakage tightness capacity. Figure 10 shows that around the openings gas flow is more important than the other parts of the external wall. At these areas we find reclosed cracks.

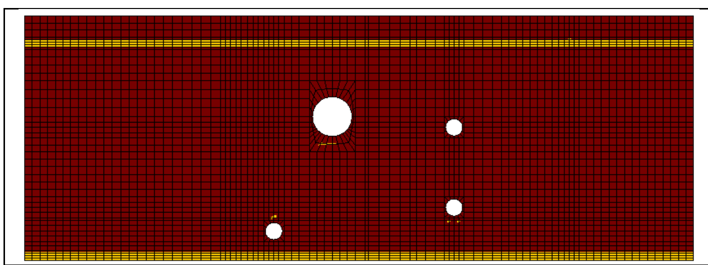

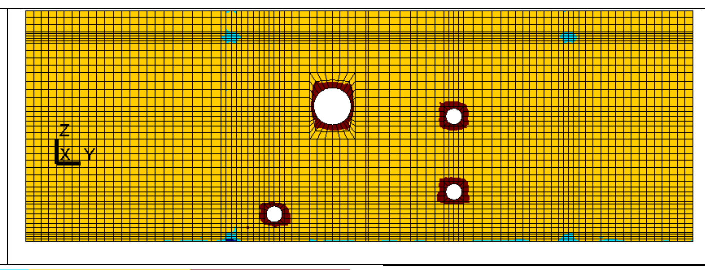

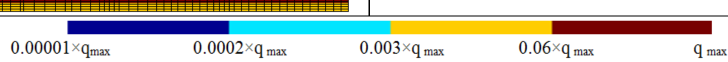

Figure 9. Normalized gas velocity (Nm/h)
Inner surface - t= 4th day of the test

Figure 10. Normalized gas velocity (Nm/h)
Outer surface - t= 4th day of the test

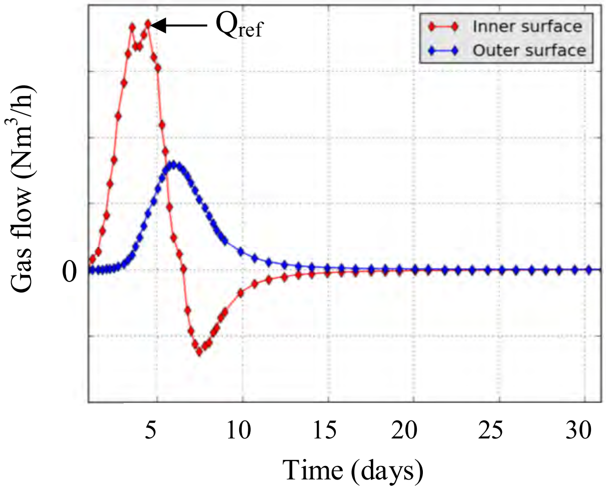

Figure 11. Surface gas flow during IT5

PARAMETER SENSITIVITY ANALYSIS

In this part parametric analyses are carried out in order to determine their influences on results. The first one concerns the value of concrete intrinsic permeability. Figure 12 indicates the evolution in results when concrete permeability is 5 times higher. On these plots Q_{ref} indicates the maximum value of flow across the inner surface, as illustrated in Figure 11. In this case the core of the wall is much more permeable. That is why all entering gas passes through the vessel's wall and leaves the vessel from the external wall. The second analysis concerns the tensile strength of concrete where two additional cases are examined: $f_{t0}/2$ and $f_{t0}/4$. From Figure 13 we can notice that maximum flow rate is almost steady, while it is multiplied by 30 when tensile strength is much lower (Figure 14). The sudden increase is essentially due to creation of cracks across the thickness of the wall around openings. For the last analysis, both permeability and tensile strength have been modified, a situation that could correspond to a very poor concrete quality. As it is illustrated in Figure 15, this time leakage is 35 times greater than the ordinary concrete reference situation. These two sensitivity analyses indicate that the knowledge of the concrete tensile strength is more important than its intrinsic permeability. In fact, gas flow through cracks is quite sensitive to their number and opening, directly linked to concrete strength as well as other parameters such as reinforcement ratio and prestressing.

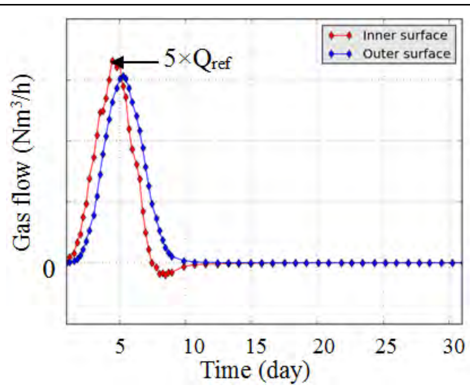

Figure 12. Higher permeable concrete ($5K_0$, f_{t0})

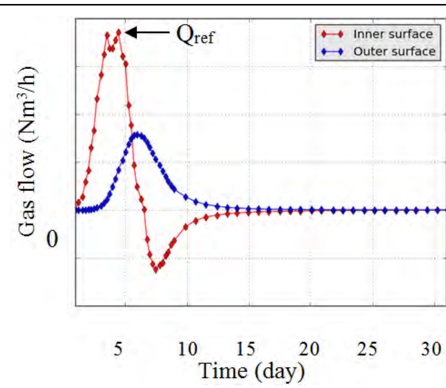

Figure 13. Low strength concrete (K_0, $0.5f_{t0}$)

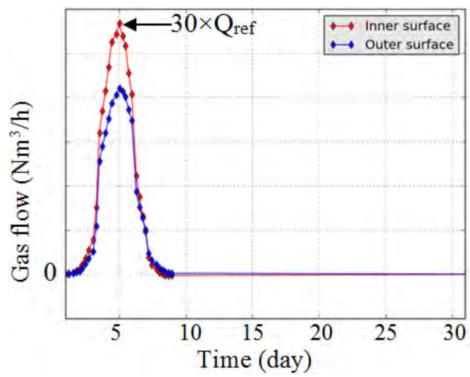

Figure 14. Lowest strength concrete (K_0, $0.25f_{t0}$)

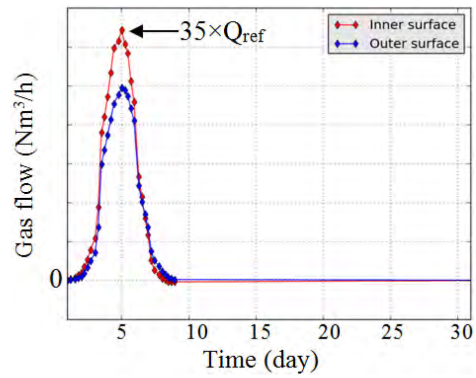

Figure 15. Poor concrete mixture ($5K_0$, $0.25f_{t0}$)

CONCLUSION

In this work, an uncoupled thermo-hydro-mechanical methodology has been developed to study the hydraulic diffusive behavior of the large-scaled concrete structures like nuclear reactor buildings, in order to predict its capacity to provide sufficient air leakage tightness. As a demonstration, the methodology is applied to the case of a containment building to determine the capacity of the model to understand its hydraulic behavior. Among various parametric studies, two of t hem are presented in this paper, and they allow measuring the sensitivity of calculated gas flows on concrete quality. First results seam to comply with in situ observations and measures and further investigations are necessary to understand the complex behavior of a PCCV and extensively validate the proposed simulation tool and study methodology. Considering the reasonable computational cost, the stability of the numerical resolution algorithm, this seems to be a promising solution for engineers in charge of studying leakage tightness of large-scale industrial structures and companies offering retrofitting solutions.

REFERENCES

Abbas, A., Carcasses, M., Ollivier, J.P. (1999). “Gas permeability of concrete in relation to its degree of saturation,” *Materials and Structures*, 32, 3-8.

Aldea, C.M., Shah, S.P, Karr, A. (1998). “Permeability of cracked concrete,” *Materials and Structures*, 32, 370-376.

Baroghel-Bouny, V., Mainguy, M., Lassabatere, T. Coussy, O. (1999). “Characterization and identification of equilibrium and transfer moisture properties for ordinary and high performance cementitious materials,” *Cement and Concrete Research*, 29, 1225-1238.

Bear, J. and Sorek, S. (1990). “Evolution of Governing Mass and Momentum Balances. Following an Abrupt Pressure Impact in a Porous Medium,” *Transport in Porous Media*, 5, 169-185.

Benboudjema F. (2002). “Modélisation des déformations différées du béton sous sollicitations biaxiales. Application aux enceintes de confinement de bâtin 0 s réacteurs des centrales nucléaires,” PhD thesis, Université de Marne-La-Vallée, France.Choınska, M., Khelidj, A., Chatzigeorgiou, G., Pijaudier-Cabot, G. (2007). “Effects and interactions of temperature and stress-level related damage on permeability of concrete,” *Cement and Concrete Research*, 37, 79–88.

Desmettre, C., Charron, J.-P. (2011). “Novel Water Permeability Device for Reinforced Concrete Under Load,” *Materials and Structures*, 44(9), 1713-1723.

Gawin, D., Pesavento, F., Schrefler, B.A. (2003). “Modelling of hygro-thermal behavior of concrete at high temperature with thermo-chemical and mechanical material degradation”, *Computational Methods in Applied Mechanics and Engineering*, 192, 1731-1771.

Gérard, B. (1996). “Contribution des couplages mécanique-chimie-transfert dans la tenue à long terme des ouvrages de stockage de déchets radioactifs,” PhD thesis, École Normale Supérieure de Cachan, France.

Granger, L. (1995). “Comportement différé du béton dans les enceintes de centrales nucléaires, Analyse et modélisation,” PhD thesis, Ecole Nationale de Ponts et Chaussées, France.

Hearn, N., Lok, G. (1998). “Measurement of permeability under uniaxial compression: a test method,” *ACI Mater J*, 95, 6, 691–4.

Jason, L. (2004). “Relation endommagement perméabilité pour les bétons application aux calculs de structures,” PhD thesis, École Centrale de Nantes et l'Université de Nantes, France.

Kermani, A. (1991). “Permeability of stressed concrete,” *Building Research and Information*, 19, 6, 360-366.

Kim J., Kwon S., Kim Y. (2006). “Analytical studies on creep of sealed concrete under multiaxial stresses using a microplane model,” *Magazine of Concrete Research*, 58, 1, 9-20.

Liu, J. (2011). “Etude experimentale de la permeabilite relative des materiaux cimentaires et simulation numerique du transfert d’eau dans le beton,” PhD thesis, Université Lille, France.

Mazars, J. (1984). “Application de la mécanique de l’endommagement au comportement non linéaire et à la rupture du béton de structure,” PhD thesis, Université Pierre et Marie Curie, France.

Mivelaz P. (1996). “Étanchéité des structures en béton armé. Fuites au travers d’un élément fissuré,” PhD Thesis, École Polytechnique Fédérale de Lausanne, Switzerland.

Monlouis-Bonnaire, J.P., Verdier, J., Perrin, B. (2003). “Prediction of the relative permeability to gas flow of cement-based materials ,” *Cement and Concrete Research*, 2333, 1-8.

Picandet, V., Khelidj, A, Bastian, G. (2001). “Effect of axial compressive damage on gas permeability of ordinary and high performance concrete”, *Cement and Concrete Research*, 31, 1525-1532.

Picandet, V., Khelidj, A., Bellegou, H. (2009). “Crack effects on gas and water permeability of concretes,” *Cement and Concrete Research*, 39, 537-547.

Souley, M., Homand, F., Pepa, S., Hoxha, D. (2001). “Damage induced permeability changes in granite :a case example at the URL in Canade”, *International Journal of Rock Mechanics and Mining Sciences*, 38, 297-310.

Sugiyama, T., Bremner, T.W., Holm T.A. (1996). “Effect of stress on gas permeability in concrete,” *ACI Mater J*, 93, 5, 443–50.

Van Genuchten, M.T. (1980). “A closed form equation for predicting the hydraulic conductivity of unsaturated soils,” *Soil Science Society of America Journal*, 44, 892-898.

Verdier, J. (2001). “Contribution à la caractérisation de l'évolution du taux de fuite des enceintes de confinement du parc nucléaire,” PhD thesis, Université Paul Sabatier de Toulouse, France.

Villain, G., Baroghel-Bouny, V., Kounkou, C., Hua, C. (2001). “Mesure de la perméabilité aux gaz en fonction du taux de saturation des bétons,” *Revue Française de Génie Civil*, 5, 2-3, 251-268.

Wang, K., Jansen, D., Shah, S.P., Karr, A. (1997). “Permeability study of cracked concrete,” *Cement and Concrete Research*, 27,3, 381-393.